sponding to that of the annealed film of chitosan A (Figure 1b). Figure 3 shows the thermal analyses on the annealed chitosan powder. The thermogravimetry (TGA) and the differential thermal analysis (DTA) were carried out with a Rigaku Thermoflex in the range 25–230 °C at a heating rate of 10 °C/min under a nitrogen atmosphere. With increasing temperature, the weight of the powder decreased rapidly until ca. 110 °C, slowly in the range 110–160 °C, and then very gradually. The DTA shows a strong endotherm until 110 °C, practically no change in the range 110–160 °C, and an endotherm at higher temperature; the latter reaction may due to a partial decomposition of the chitosan. These results indicate that all water molecules included in the annealed chitosan powder are removed at 110 °C. Therefore, an X-ray analysis was done with the annealed chitosan powder having no water molecules. Immediately after drying under vacuum at 110 °C for 7 h, the annealed chitosan powder was X-rayed under vacuum. The resultant powder pattern was just the same as that of the undried powder. Furthermore, the fiber pattern of the annealed chitosan A film (Figure 1b) did not change under the same conditions of drying the film as for the annealed chitosan powder. From these results, it is clear that the unit cell does not have any water molecules. The calculated density, 1.52 g cm^{-3}, is lower than that of cellulose (around 1.62 g cm^{-3}). This may be due to the presence of the primary amino group in chitosan.

Averbach[12] reported that chitosan appears to have an atomic arrangement similar to that of chitin. The position of the (020) peak (*c* is the fiber axis) depended on the water content and was lowered on drying at 134 °C. It was postulated that water molecules are loosely bound between the chitosan chains along the [010] direction.

In contrast, our annealed chitosan showed no (020) reflection and had a strong (120) reflection which was not observed in the tendon chitosan and was very weak in our chitosan film before annealing. With increasing annealing temperature, the intensity of the former reflection, which was strong before annealing (Figure 1a), decreased and that of the latter increased. Except for this, both chitosans showed similar equatorial reflections. As with (1→3)-α-D-glucan and other polysaccharides,[5–10] it is difficult to consider that annealing produced any drastic change in the chain packing of chitosan since the chitosan film did not show any appreciable change during annealing even though this is an irreversible process. Furthermore, the *a*- and *b*-axis lengths of our annealed chitosan are a little smaller than those of the tendon chitosan.[2]

These observations lead to the following proposal on the chitosan conformation in the present new polymorph. There seems to be only a small difference in chain packing between the tendon chitosan cell and our annealed cell, that is, the presence or absence of water molecules. Upon removal of loosely bound water molecules between the chains along the [010] direction in the tendon chitosan, new interchain hydrogen bonds may be formed. The present new polymorph of chitosan is energetically more stable than that of the tendon chitosan. Further analysis is under way.

Acknowledgment. We are indebted to Dr. Noboru Tohge, Department of Applied Chemistry, Faculty of Engineering, University of Osaka Prefecture, for providing the thermal analysis data.

References and Notes

(1) Muzzarelli, R. A. A. "Chitin"; Pergamon Press: Oxford, 1977.
(2) Clark, G. L.; Smith, A. F. *J. Phys. Chem.* **1937**, *40*, 863.
(3) Darmon, S. E.; Rudall, K. M. *Discuss. Faraday Soc.* **1950**, 251.
(4) Samuels, R. J. *J. Polym. Sci., Polym. Phys. Ed.* **1981**, *19*, 1081.
(5) Marchessault, R. H.; Deslandes, Y.; Ogawa, K.; Sundararajan, P. R. *Can. J. Chem.* **1977**, *55*, 300.
(6) Ogawa, K.; Misaki, A.; Oka, S.; Okamura, K. *Carbohydr. Res.* **1979**, *75*, C13.
(7) Ogawa, K.; Okamura, K.; Yui, T.; Watanabe, T.; Takeo, K. *Carbohydr. Polym.* **1983**, *3*, 287.
(8) Tvaroska, I.; Ogawa, K.; Deslandes, Y.; Marchessault, R. H. *Can. J. Chem.* **1983**, *61*, 1608.
(9) Ogawa, K.; Mizuno, T.; Miyanishi, T.; Yui, T.; Watanabe, T. *Abstr. Annu. Meet. Agric. Chem. Soc. Jpn.* **1983**, 317.
(10) Ogawa, K.; Hara, C.; Kiho, T.; Ukai, S.; Yui, T.; Miyanishi, T.; Watanabe, T., unpublished data.
(11) Hirano, S.; Yamaguchi, R. *Biopolymers* **1976**, *15*, 1685.
(12) Averbach, B. L. Report MITSG 75-17, National Technical Information Service, U.S. Department of Commerce, 1975.

Kozo Ogawa*
Radiation Center of Osaka Prefecture
Shinke-cho, Sakai, Osaka 593, Japan

Shigehiro Hirano
Department of Agricultural Biochemistry
Tottori University
Tottori 680, Japan

Toshio Miyanishi, Toshifumi Yui, and Takehiko Watanabe
College of Agriculture
University of Osaka Prefecture
Sakai, Osaka 591, Japan

Received June 28, 1983

Chloride Ion Conductivity in a Plasticized Quaternary Ammonium Polymer

Solvent-free polymer electrolytes[1,2] have generated much interest owing to their possible use in high energy density batteries. Most research in this area has focused on alkali metal ion conduction in solid electrolytes formed by alkali metal salts and poly(ethylene oxide)[3] or poly(propylene oxide).[2] Although cation transport has been substantiated by use of reversible cation electrodes, i.e., alkali metals,[4–6] intercalates,[1] and sodium amalgam,[7] charge transport by anions may be substantial.[5,6] Here we report the first studies of fast anion conduction in solid polymer electrolytes, poly(diallyldimethylammonium chloride) (I, DDAC) plasticized with poly(ethylene glycol) (II, PEG; average MW = 300). In these anhydrous electrolytes, the positive charge is anchored in the polymer backbone. Thus the dc electrical properties displayed by these conductors are clearly attributable to the anion.

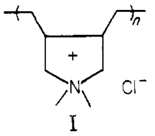

I

$HO\text{-}(CH_2CH_2O)_n\text{-}H$

$n \sim 6$

II

An important motivating factor for the use of DDAC is that the positive quaternary nitrogen is surrounded by four alkyl groups, thus separating the opposite charges and reducing tight ion pairing. Tight ion pairing has been shown to significantly reduce the mobility of charge carriers in solid polymer electrolytes.[8]

Use of plasticizers in polymers is known to increase polymer chain flexibility, increase free volume, and decrease the glass transition temperature, T_g. These changes are also known to increase ionic conductivity in solid electrolytes.[9,10] Therefore, the present research was designed to investigate the possibility that plasticizers might increase the ionic conductivity of the polyelectrolyte DDAC.

0024-9297/84/2217-0975$01.50/0

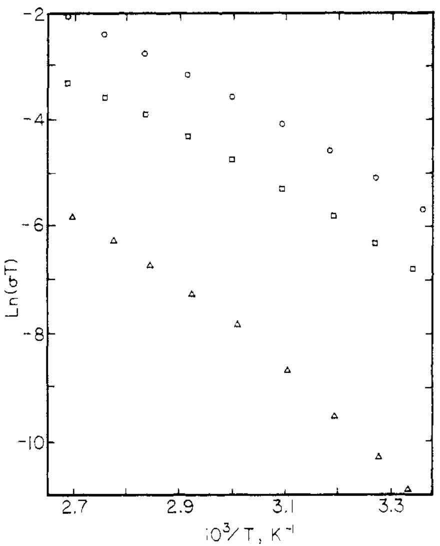

Figure 1. Ionic conductivity, σ (Ω^{-1} cm^{-1}), vs. temperature plotted as ln (σT) vs. $1000/T$ for various mole ratios of chloride ion in polymer to hydroxyl group in plasticizer: (△) 2:1; (□) 1:1; (○) 0.67:1.

The conductivity, σ, of pure, brittle DDAC at 25 °C was not measurable on our instruments, which indicates a conductivity much less than 10^{-9} Ω^{-1} cm^{-1}. A number of esters and ethers were tested for compatibility as plasticizers. Brittle, cloudy-white films resulted when mixtures of DDAC with diisodecylphthalate, dibutyl phthalate, dibutyl sebacate, tetraethylene glycol dimethyl ether, poly(ethylene oxide), or poly(vinyl alcohol) (88% hydrolyzed) were cast from methanol or methanol/water solutions at 25 or 60 °C. Segregation of the plasticizer also occurred in same cases. The only plasticizer found to be effective was PEG (average MW = 300). Since the similar compound tetraethylene glycol dimethyl ether was imcompatible, the hydroxyl groups on the polyether must play an important role in the plasticizing interaction. This hypothesis is substantiated by IR spectroscopy, which shows that the O–H stretch for pure PEG is lowered from ~3400 to ~3240 cm^{-1} when PEG is mixed with DDAC in a ratio of one hydroxyl group per two chloride ions. This behavior suggests hydrogen bonding to the more electronegative chloride ion in preference to hydrogen bonding with the oxygen such as found in pure PEG. Evidence for similar plasticizing behavior has been reported for sodium styrenesulfonate groups and glycerol.[11]

Standard inert-atmosphere techniques were used in the preparation and study of these electrolytes because water appears to displace the glycol from the plasticized polymer. After preparation from nominally dry materials, the last traces of water were removed by vacuum drying of films. Infrared spectra on thick films of these samples in the 1630-cm^{-1} region indicate that the water content is below 100 ppm. Judging from infrared spectra, the samples quickly absorb water when exposed to atmospheric moisture. Films with 0.32, 0.48, and 0.58 weight fractions of PEG were made and these correspond to mole ratios of chloride ion to hydroxyl group of 2, 1, and 0.67, respectively. These films are clear and flexible at room temperature. Differential scanning calorimetry (20 °C/min) indicates that T_g is -37 ± 2 °C for all three mole ratios. No endotherms are observed for the melting of pure PEG in these electrolytes. Polarized optical microscopy also indicates that the films are amorphous.

Ac complex impedance data collected over the frequency range of 10 Hz to 500 kHz with platinum ion-blocking electrodes were used to calculate bulk conductivity of samples. The variable-temperature electrical conductivity data yield curved plots of ln (σT) vs. $1/T$, Figure 1. This behavior, which is similar to that of diffusion of small molecules through polymers, has been seen previously for other polymer electrolytes.[2,12] Transport of ions in these materials may be described by WLF-type equations rather than the Arrhenius law.[2,10,13] Conductivity increases as the amount of plasticizer in the electrolyte increases; see Table I. (The plasticizer, which was purified by passage through ion-exchange resins in H$^+$ and OH$^-$ forms, displayed negligible conductivity, so the influence of the plasticizer did not arise from impurities.)

Table I

mole ratio Cl$^-$:hydroxyl	conductivity, Ω^{-1} cm^{-1} 26 °C	98 °C
2:1	7×10^{-8}	1×10^{-5}
1:1	4×10^{-6}	1×10^{-4}
0.67:1	1×10^{-5}	3×10^{-4}

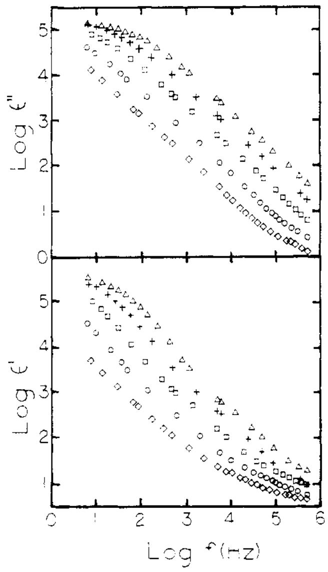

Figure 2. Plots of log dielectric constant, ϵ', and log dielectric loss, ϵ'', vs. log frequency in Hertz for the 2:1 chloride to hydroxyl electrolyte at various temperatures: ◇, 26 °C; ○, 41 °C; □, 60 °C; +, 79 °C; △, 98 °C.

Plots of ϵ' and ϵ'' vs. frequency with ion-blocking electrodes are shown in Figure 2. As frequency decreases, interfacial polarization of the ionic conductor increases, which results in a continuously increasing dielectric constant, as has been predicted by theory[14] and has been reported for inorganic solid electrolytes.[15,16] Therefore, the reported dielectric constants are due to double-layer capacitances rather than molecular dipoles. According to the theory,[14] at low frequencies the internal field of the electrolyte equally opposes the applied field and no further polarization occurs, so the ϵ' curve flattens out. The beginning of this behavior is seen in the high-temperature plot. The absence of maxima in the ϵ'' plots, above 10 Hz, in conjunction with other data indicates that the frequency response over the frequency range studied is due to ion motion rather than molecular relaxations such as the rotation of an –OH group. High dielectric constants also have been reported for solid electrolytes formed between poly(ethylene oxide) and alkali metal salts.[17]

Complex impedance plots are typical of those seen for ionic conductors with ion-blocking electrodes, Figure 3A. In particular, the spur found at low frequencies is ascribed to double-layer capacitance in a cell with an ion-blocking electrode configuration.[18]

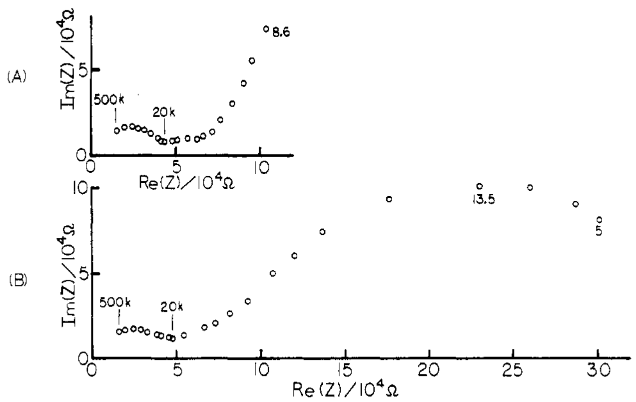

Figure 3. Plots of the imaginary part vs. the real part of the impedance (Z) for the 2:1 chloride: hydroxyl electrolyte at 60 °C. Frequencies (5 Hz to 500 kHz) are listed next to the data points. (A) With Pt electrodes; (B) with Hg/Hg_2Cl_2, calomel, electrodes.

To provide a definitive assignment of the low-frequency spur, calomel electrodes were employed in a second set of complex impedance expts. The spur seen previously for ion-blocking electrodes is now converted to an arc, Figure 3B. According to impedance/frequency response theory,[18] this arc can be ascribed to charge-transfer resistance at the chloride ion reversible electrode. This type of response is well characterized for other polymer electrolyte systems with cation reversible electrodes.[5,6]

The present work demonstrates that conductivity due to anion transport in a solvent-free polymer system can be on the same order of magnitude as that found for poly(ethylene oxide)–alkali metal salt systems. The electrical properties characterized in the present system may be attributed solely to the anion since the positive countercharge is anchored in the polymer backbone.

Acknowledgment. This research was partially supported by a grant from the Office of Naval Research. L.C.H. was the recipient of a DOE summer research fellowship administered by the Electrochemical Society. We appreciate helpful discussions with M. A. Ratner.

Registry No. Poly(diallyldimethylammonium chloride), 26062-79-3; poly(ethylene glycol), 25322-68-3; chloride, 16887-00-6.

References and Notes

(1) Armand, M. B. "Proceedings of the Workshop on Lithium Nonaqueous Battery Electrochemistry", Cleveland, Ohio, June 1980, pp 261–270.
(2) Armand, M. B.; Chabagno, J. M.; Duclot, M. J. In "Fast Ion Transport in Solids"; Vashishta, P., Mundy, J. N., Shenoy, G. K., Eds.; North-Holland Publishing Co.: New York, 1979; pp 131–136.
(3) Wright, P. V. *Br. Polym. J.* **1975**, *7*, 319–327.
(4) Weston, J. E.; Steele, B. C. H. *Solid State Ionics* **1982**, *7*, 75–79.
(5) Weston, J. E.; Steele, B. C. H. *Solid State Ionics* **1982**, *78*, 81–88.
(6) Sørensen, P. R.; Jacobsen, T. *Electrochim. Acta* **1982**, *27*, 1671–1675.
(7) Dupon, R. W.; Whitmore, D. H.; Shriver, D. F. *J. Electrochem. Soc.* **1981**, *128*, 715–717.
(8) Dupon, R. W.; Papke, B. L.; Ratner, M. A.; Whitmore, D. H.; Shriver, D. F. *J. Am. Chem. Soc.* **1982**, *104*, 6247–6251.
(9) Killis, A.; LeWest, J.-F.; Cheradame, H.; Gandini, A. *Makromol. Chem.* **1982**, *183*, 2835–2845.
(10) Papke, B. L.; Ratner, M. A.; Shriver, D. F. *J. Electrochem. Soc.* **1982**, *129*, 1694–1701.
(11) Lundberg, R. D.; Makowski, H. S.; Westerman, L. In "Ions in Polymers"; Eisenberg, A., Ed.; American Chemical Society: Washington, D.C., 1980; pp 67–76.
(12) Stainer, M.; Hardy, L. C.; Whitmore, D. H.; Shriver, D. F. *J. Electrochem. Soc.*, in press.
(13) Arai, K.; Eisenberg, A. *J. Macromol. Sci., Phys.* **1980**, *B17*, 803–832.
(14) Lines, M. E. *Phys. Rev. B: Condens. Matter* **1979**, *19*, 1189–1195.
(15) Armstrong, R. D.; Taylor, K. *J. Electroanal. Chem.* **1975**, *63*, 9–17.
(16) Hodge, I. M.; Ingram, M. D.; West, A. R. *J. Am. Ceram. Soc.* **1976**, *59*, 360–366.
(17) Fontanella, J. J.; Wintersgill, M. C.; Calame, J. P.; Andeen, C. G. *Solid State Ionics* **1983**, *8*, 333–339.
(18) Macdonald, J. R. *J. Chem. Phys.* **1974**, *61*, 3977–3996.

Leslie C. Hardy and Duward F. Shriver*
Department of Chemistry and Materials Research Center
Northwestern University, Evanston, Illinois 60201

Received November 29, 1983

Ethylene Units in $Al(CH_3)_3$-Cocatalyzed Polymerization of 3-Methyl-1-pentene

As reported in a previous paper,[1] ^{13}C-enriched C_2H_4 comonomer units have been detected in poly(3-methyl-1-pentene) prepared in the presence of the catalytic system δ-$TiCl_3/Al(^{13}CH_3)_3/Zn(^{13}CH_3)_2$

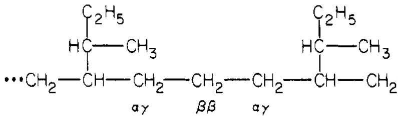

$$\cdots CH_2-CH(CH(CH_3)C_2H_5)-CH_2-CH_2-CH_2-CH(CH(CH_3)C_2H_5)-CH_2\cdots$$

Two weak resonances of similar intensity have been detected in the ^{13}C NMR spectrum of this polymer (Figure 1) at 21.5_5 and 27.6_0 ppm for $\beta\beta$[2,3] and $\alpha\gamma$ (enriched) methylene carbons. The reason for the similar intensity of the $\beta\beta$ and $\alpha\gamma$ resonances in Figure 1 is that the $\alpha\gamma$ resonance from 3-methyl-1-pentene units is so low as to go undetected. In principle, a small amount of 1-^{13}C-enriched C_2H_4 could appear in the system and copolymerize as a consequence of metathesis involving ^{13}C-enriched metallocarbenes and 3-methyl-1-pentene.

$$\begin{array}{c} Mt{=}^{13}CH_2 + CH_2{=}CH\text{-}CH(CH_3)C_2H_5 \\ \uparrow\downarrow \\ Mt{=}CH\text{-}CH(CH_3)C_2H_5 + CH_2{=}^{13}CH_2 \end{array} \qquad (1)$$

It may be worthwile to mention that metallocarbenes have been suggested to play a role even in olefin insertion.[4] On the other hand, one could conjecture that 1,2-^{13}C-enriched C_2H_4 results from decomposition of two Mt–$^{13}CH_3$ bonds through a more or less complicated reaction pathway,[5] e.g.

$$2Mt\text{–}^{13}CH_3 \rightarrow {}^{13}CH_2{=}{}^{13}CH_2 + \text{decomposition products} \qquad (2)$$

In principle, one could discriminate between the presence of either 1-^{13}C-enriched ethylene or 1,2-^{13}C-enriched ethylene by observing the ^{13}C–^{13}C satellites. However, the relatively low enrichment (30%) of the $Al(CH_3)_3$ and $Zn(CH_3)_2$ used,[1] as well as the low content of C_2H_4 in the polymer, precludes such a possibility. On the other hand, when 1-^{13}C-enriched 3-methyl-1-pentene is polymerized in the presence of δ-$TiCl_3/Al(CH_3)_3/Zn(CH_3)_2$, 1-$^{13}C$-enriched C_2H_4 is still expected by metathesis, while unenriched ethylene is expected from the decomposition reaction.

The spectrum of poly-(3-methyl-1-pentene-*1*-^{13}C) prepared with δ-$TiCl_3/Al(CH_3)_3$ is reported in Figure 2. It may be observed that the resonance at 27.5_7 ppm ($\alpha\gamma$-methylene carbons) is still present while that at 21.5_5 ppm has disappeared. This is just what one would expect from the presence of unenriched ethylene units. As a matter of fact, the $\alpha\gamma$-enriched methylene carbons can arise either

0024-9297/84/2217-0977$01.50/0